ELSEVIER

Thermochimica Acta 361 (2000) 131–138

thermochimica acta

www.elsevier.com/locate/tca

The structure of bone studied with synchrotron X-ray diffraction, X-ray absorption spectroscopy and thermal analysis

Fabian Peters, Karsten Schwarz, Matthias Epple*

Solid State Chemistry, Faculty of Chemistry, University of Bochum, D-44 780 Bochum, Germany

Received 18 November 1999; accepted 1 February 2000

Abstract

Bone samples of different origins and two bone substituent materials were studied with modern solid-state chemical methods: combined thermogravimetry–differential thermal analysis–mass spectrometry (TG-DTA-MS), X-ray powder diffraction (synchrotron), X-ray absorption spectroscopy (EXAFS, Ca K-edge, synchrotron), and infrared spectroscopy. The results complement those from medical histology. The mineral phase consists of disordered apatite with no indication for another calcium phosphate phase. Size and morphology of the bone mineral particles are independent of the nature of the bone sample, but there are significant differences in the overall composition of the bone samples and in the carbonate content of the mineral phase. It is concluded that the biological resorption of living bone (remodeling) is closely related to morphology and composition of its mineral phase. © 2000 Elsevier Science B.V. All rights reserved.

Keywords: Calcium phosphate; Bone; Biomineralization; EXAFS spectroscopy; X-ray diffraction

1. Introduction

Bone is one of the most important biological structures in the field of biomineralization [1,2]. From the viewpoint of a materials scientist, bone is a composite of an organic and an inorganic phase with highly hierarchical structure [3,4]. Its main building blocks are long collagen fibrils of about 100-nm diameter that contain nanometer-sized carbonated apatite crystals (‘dahllite’). There is a clear relationship between the weight fraction of the mineral phase in bone and its mechanical properties [4]. The skeletal system in vertebrates is subject to continuous dissolution and formation (‘remodeling’) by osteoclasts and osteoblasts.

Most of our knowledge about structure and size of the bone mineral comes from transmission electron microscopy (TEM) [5–7], a method that requires previous destruction of the original bone structure. Furthermore, many studies of bone were made with just one or two methods, and the comparison between the results of different methods is difficult as this biological material naturally shows a wide variation in its properties depending on its history and origin.

It was the aim of this study to apply a number of modern solid-state chemical techniques to four histologically well-characterized bone samples. As it is not known how chemical or mechanical treatment changes the ultrastructure of bone, we decided to study the original bone samples after minimal treatment with non-destructive methods. We are aware that this method stands in contrast to standard medical analysis where soft tissue is usually removed, but it appeared to be more appropriate for a comparative

* Corresponding author. Tel.: +49-234-322-4151; fax: +49-234-3214-558.
E-mail address: matthias.epple@ruhr-uni-bochum.de (M. Epple).

0040-6031/00/$ – see front matter
PII: S0040-6031(00)00554-2

study of this complex material. Additionally, two clinical bone substituent materials were studied: sterilized and chemically treated bovine bone: Kiel bone ('Kieler Knochenspan') and calcined bovine bone: endobon®. Three questions were addressed in this study:

1. How does the overall composition vary in different bone samples?
2. Is there a change in structure and morphology of the primary mineral particles?
3. What are the differences between natural bone and the two bone substitution materials?

2. Experimental

Four bone samples that would have remained useless after completed medical diagnosis (histology) from patients treated at the University Hospital Hamburg (Eppendorf) were studied. The sample size was about 0.5 cm^3 in all cases.

For better readability, the samples are denoted in the text as follows (registration numbers at the Department of Bone Pathology, University of Hamburg, Prof. Delling, are also given):

- Cancellous bone (healthy spongiosa) from femoral head of Case 988/98 (female, 66 years): 'spongiosa A'
- Cancellous bone (healthy spongiosa) from distal femur of Case 1462/98 (male, 12 years): 'spongiosa B'
- Newly formed callus bone after fracture from distal femur of Case 1462/98: 'callus bone'
- Cancellous bone (spongiosa) with osteoblastic osteosarcoma from distal femur of Case 1462/98. Tumor bone was formed in between the trabecular structures of the spongiosa: 'tumor bone'

Histology was performed after embedding in poly(-methylmethacrylate) and cutting into 5-μm thin sections. For light microscopy, all biopsies were stained with toluidine blue and von Kossa stain. For diffraction, EXAFS and infrared spectroscopy, the bone samples were rinsed with ethanol, dried in vacuo at room temperature and ground in an agate mortar. For thermogravimetry, the samples were only dried in vacuo to remove adsorbed water.

Endobon® consists of calcined bovine spongiosa (two-step calcination process: >700 and >1000°C) [8,9]. It was obtained from Merck Biomaterial, Darmstadt, Germany. Kiel bone ('Kieler Knochenspan') is a clinical bone substituent material that is not in use anymore. It consists of bovine spongiosa that is first mechanically cleared of bone marrow, followed by extraction with $CHCl_3/CH_3OH$ and treatment with H_2O_2 [10]. Synthetic hydroxyapatite was purchased from Merck, Darmstadt.

Fourier transform IR-spectroscopy was carried out with a Perkin–Elmer PE 1720 instrument in KBr pellets. Combined thermogravimetry–differential thermal analysis–mass spectrometry (TG-DTA-MS) was carried out on a Netzsch STA 409/Balzers QMS 421 system (sample mass: 71 to 91 mg; open alumina crucibles; 30–1000°; 10 K min^{-1}; dynamic air atmosphere; 50 ml min^{-1}).

X-ray absorption spectroscopy (EXAFS) was carried out at the Hamburger Synchrotronstrahlungslabor (HASYLAB) at Deutsches Elektronen-Synchrotron (DESY), Hamburg, at beamline E4 (EXAFS II). Experiments were performed at the calcium K-edge (ca. 4042 eV) in transmission mode at room temperature. A few milligrams of ground samples were put on adhesive tape that was then brought into the beam. For data evaluation, the programs AUTOBK, FEFFIT [11] and FEFF 5.04 [12] were used. Hydroxyapatite, $Ca_{10}(PO_4)_6(OH)_2$, has a hexagonal crystal structure with two crystallographically independent calcium positions where the first position (Ca_1) is occupied by four calcium atoms per unit cell and the second (Ca_2) by six calcium atoms per unit cell [13]. The coordination number that is detected by EXAFS spectroscopy is composed of the weighted sum of both crystallographic environments (0.4 Ca_1+0.6 Ca_2). Higher shells of light backscatterers (e.g. oxygen) were omitted due to small intensity and shells in very close neighborhood were combined in order to keep the number of fit parameters manageable and mathematically significant. Multiple scattering pathways were of negligible magnitude. EXAFS data were Fourier transformed in the range of k=2–9 $Å^{-1}$ using k^3 weighting of the data. Fitting was performed in r-space in the range of r=1.2–5.8 Å. In general, at least two scans were recorded for each sample. The coordination number for each shell was fixed to the value of crystalline

hydroxyapatite. The amplitude reduction factor S_0^2 was fixed to 1.

X-ray powder diffraction was carried out at beamline B2 at HASYLAB/DESY. The samples were measured at room temperature in rotating 1.0-mm glass capillaries in the Debye–Scherrer mode with a wavelength of 120.06 pm. Soller slits were placed between sample and detector. Data were collected for $8<2\Theta<42^\circ$ in steps of 0.01 with a counting time of ca. 6 s at each point (scintillation counter).

3. Results

In order to determine the overall composition of the bone samples, we have carried out combined TG-DTA-MS in dynamic air atmosphere. The general features as displayed by all compounds can be seen in Fig. 1 where the curve for tumor bone is shown. The sample loses weight in three steps. The first step occurs from 50 up to about 260°C (water; signal at m/z=18). In the second step, up to about 600°C, the organic components (bone marrow, fat tissue, collagen) are pyrolyzed and burnt (combustion products water and carbon dioxide, m/z=44, and organic fragments, e.g. methyl, m/z=15). In the third step, between 650 and 850°C, carbon dioxide released from carbonated apatite [14,15] is detected. We have defined the bone mineral content (carbonated apatite) as the relative mass remaining after heating to 600°C.

The composition of the four bone samples and the two bone substituent materials is highly variable (Table 1). As expected from histology, tumor bone is much higher mineralized than spongiosa. Callus bone and Kiel bone are in-between these two extremes. The content of water is mostly constant in all samples, except for endobon.

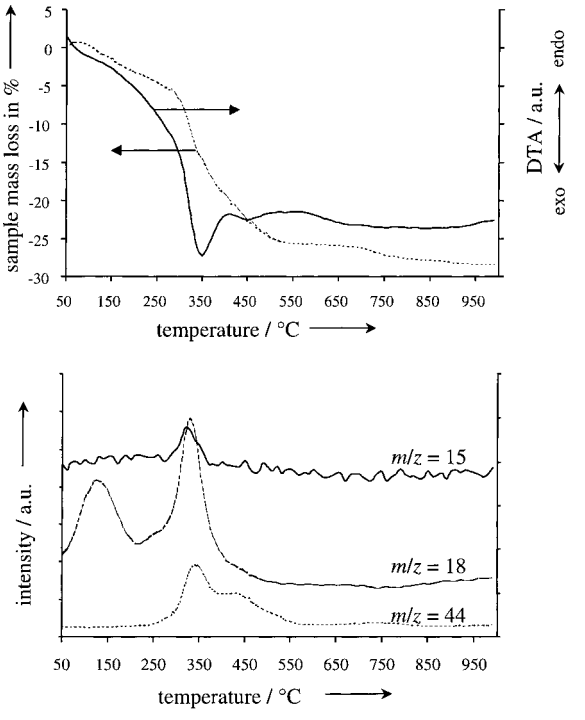

Fig. 1. Combined thermogravimetry–differential thermal analysis–mass spectrometry on tumor bone (dynamic air atmosphere). The sample is losing weight in three steps: 50–260°C (water, m/z=18); 260–600°C (combustion of organic matrix, m/z=15, 18, 44 and others); and 650–850°C (decarboxylation of carbonated apatite, m/z=44). Dashed line, relative sample mass; and solid line: DTA signal.

Table 1
Composition of the bone samples and the bone substituent materials, as derived from thermogravimetry[a]

	H_2O (wt.%)	Soft tissu+organic bone matrix (wt.%)	Mineral phase (wt.%)	Content of $CaCO_3$ (wt.%)	Content of apatite (wt.%)	Ratio apatite: $CaCO_3$ (w:w)
Callus bone	6.9 (9)	47.7 (3)	45.4 (8)	1.4 (14)	44.0 (16)	31
Tumor bone	5.7 (10)	21.2 (15)	73.1 (5)	5.2 (9)	67.9 (10)	13
Spongiosa A	5.7	57.9	36.4	2.4	34.0	14
Spongiosa B	5.4 (6)	68.4 (6)	26.3 (2)	0.6 (2)	25.7 (3)	37
Kiel bone	7.8 (10)	28.7 (13)	63.5 (3)	3.7 (4)	59.8 (5)	16
Endobon	0.0	0.0	100.0	0.0	100.0	–

[a]Only one run was possible for spongiosa A due to small sample amount. Standard deviations are given in parentheses. The mineral content (i.e. carbonated apatite) was defined as the remaining mass after heating to 600°C under air. The content of carbonate was computed from the weight loss between 600 and 1000°C. Note that the formulation of the carbonate content in the carbonated apatite as '$CaCO_3$' is purely formal, and that $CaCO_3$ is not present as a discrete phase.

If we formulate the composition of carbonated apatite as $Ca_{10}(PO_4)_6(OH)_2 \cdot x\, CaCO_3$, we can compute the ratio of calcium phosphate $Ca_{10}(PO_4)_6(OH)_2$ to calcium carbonate $CaCO_3$ from the TG data, using the ratio of the total mineral content and the content of CO_2 (computed from the weight loss between 600 and 1000°C). Note that carbonate ions are incorporated into the apatite lattice, i.e. $CaCO_3$ is not present as a discrete phase. The relative carbonate content is strongly variable, ranging from ca. 13:1 in tumor bone to ca. 37:1 in spongiosa B. With this limited database, conclusions cannot be drawn about the dependence of the carbonate content of bone on its origin. However, it was postulated in the literature from infrared spectra that mature bone contains less carbonate than 'young' bone [16,17]. Tumor bone is a comparatively fast-growing hard tissue. Apparently, nature prepares bone mineral with different chemical composition. Thermal analysis appears to be well suited to study overall bone composition.

Endobon did not lose mass during the experiment, as it was prepared by calcination at 1000°C. Together with the diffractometric data (see below), this indicates that endobon consists of pure hydroxyapatite without any carbonate content as all the CO_2 was released during synthesis.

X-ray powder diffraction was carried out at a synchrotron source where the photon flux is much higher and the instrumental peak broadening is smaller than with conventional X-ray sources (Fig. 2). The following facts are immediately observable:

- All samples consist of hydroxyapatite, albeit with different crystallite size as indicated by the peak width.
- There is no visually detectable difference between the two bone samples and Kiel bone; therefore, the mineral phase is unchanged even after the rigorous treatment of Kiel bone.
- Endobon consists of highly crystalline hydroxyapatite with even higher crystallinity than synthetic hydroxyapatite. It contains a foreign phase that was identified as calcium oxide (CaO) that remained after decarboxylation of carbonated apatite.
- The organic matrix (e.g. collagen) does not show up in wide-angle X-ray diffractometry.

A semi-quantitative relationship between peak width and crystallite size D (diameter of the coherently scattering domains) is given by the Scherrer equation [18]. However, structural disorder and strain phenomena (e.g. caused by carbonate substitution) can also induce peak broadening [18]. As bone mineral contains a considerable amount of carbonate, it is clear that the values obtained here and elsewhere can only be indicators for the particle size, but do not constitute accurate values. Note that the diffraction peak pairs

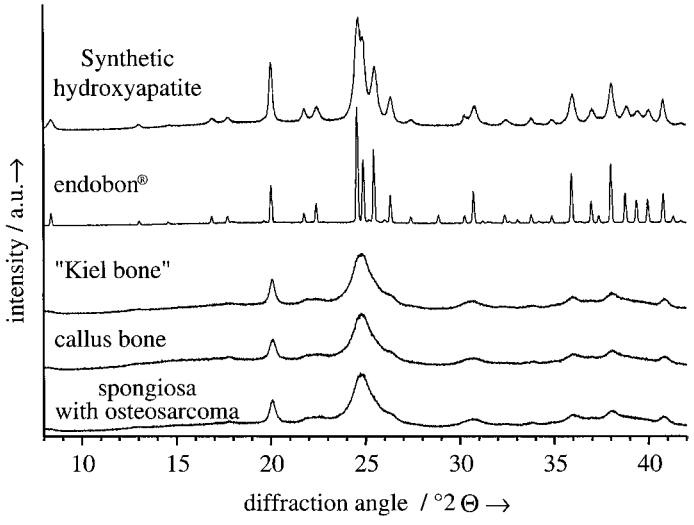

Fig. 2. X-ray powder diffractograms (synchrotron radiation) of two natural bone samples, of two bone substituent materials, and of synthetic hydroxyapatite.

Table 2
Average crystallite size D (nm) as determined from high-resolution X-ray powder diffractograms using the Scherrer equation

Diffraction line index	(1 1 1)	(0 0 2)	(2 1 0)/ (1 2 0)	(1 3 0)/ (3 1 0)	(1 1 3)	(2 2 2)	(2 1 3)/ (1 2 3)	(0 0 4)
Diffraction angle (2Θ, in degrees)	17.8	20.1	22.4	30.8	33.9	36.0	37.0	40.9
Callus bone	19	20	10	8	21	15	12	18
Tumor bone	23	21	11	8	17	16	12	18
Kiel bone	18	22	9	7	20	16	13	20
Hydroxyapatite (synthetic)	29	36	24	26	34	22	28	34
Endobon	>71	>64	>67	>63	>64	>62	>64	>64

(210)/(120), (130)/(310) and (213)/(123) have identical lattice spacing, respectively, in pure hydroxyapatite, therefore they can be treated as single peaks. Carbonate incorporation does not lead to symmetry reduction that would lead to peak-splitting [14,19].

Table 2 lists the computed values for D for all examined samples. Within the error limit associated with this evaluation procedure, the two bone samples and Kiel bone are identical. Interestingly, synthetic hydroxyapatite consists of very small crystallites as well. The diffraction line widths for endobon are at the limit of instrumental resolution, therefore we can compute only a lower limit for the crystallite size.

The bone samples exhibit a pronounced anisotropy in crystallite size. In cases where the third Miller index l is zero, the crystallite size is smaller than with the other peaks (about 10 nm compared to about 20 nm). This indicates an elongation of the crystallites in the crystallographic c-direction, a fact already discovered by electron diffraction on single-bone mineral particles [6]. This anisotropy is not found in synthetic hydroxyapatite. The results correspond well to earlier studies on bone ca. 4*20 nm [20–23]; dentine ca. 4*20 nm [21]; and calcium phosphate concretions in the pineal gland ca. 10*35 nm [24]. Apparently, biological apatite is always found with the same crystallite size and shape, regardless of its origin.

The application of synchrotron radiation was essential in this case. We have taken X-ray diffractograms of bone samples with conventional diffractometers and found a considerably worse resolution. Small peaks (as for the CaO in endobon) and broad peaks (as for spongiosa) cannot be reliably detected, let alone quantitatively evaluated.

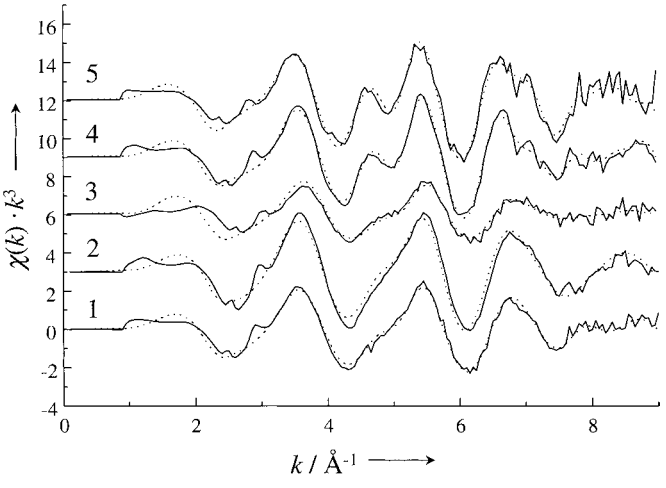

Fig. 3. EXAFS function $\chi(k)$ of five samples, recorded at the Ca K-edge. A fine structure due to higher shells is visible for well-crystallized samples (especially at 4.5 $Å^{-1}$). The main oscillations representing the Ca–O environment are similar in all samples (solid lines, experimental data; and dotted lines, fit to the data). 1, Tumor bone; 2, callus bone; 3, Kiel bone; 4, endobon; and 5, synthetic hydroxyapatite.

Diffraction techniques are sensitive only to ordered (crystalline) structures. For disordered, nanocrystalline, or amorphous samples, X-ray absorption spectroscopy (EXAFS) is better suited to yield quantitative information on the short-range environment (a few Å) around selected elements [25]. We have carried out EXAFS at the calcium K-edge, giving the local environment of calcium up to ca. 8-Å distance. The results are shown in Figs. 3 and 4. Visually, there is almost no difference between the bone samples and Kiel bone. However, there is a difference to the purely 'inorganic' materials hydroxyapatite and endobon if higher coordination spheres (>2.5 Å) are considered. The amplitude of the Fourier transform magnitude is much smaller for these shells whereas it is comparable for the first calcium-oxygen shell. This points to a substantially higher disorder in the biological samples that is ascribed to static disorder due to carbonate substitution and small crystallite size.

Quantitative fits to the data show that the biological samples consist of disordered hydroxyapatite as all apatite shells can be well fitted (Table 3). This is in good agreement with the only available EXAFS study on (mouse) bone [26], as well as studies on amorphous calcium phosphate (ACP) [27,28] that is discussed as a precursor in initial bone formation [16], and on crystalline hydroxyapatite [27–30]. There is no indication for other calcium phosphate phases (e.g. octacalcium phosphate — OCP).

The calcium-neighbor distance is mostly constant in bone samples, hydroxyapatite and endobon, but the Debye–Waller factor σ^2 is higher in bone samples, indicating greater disorder. It must be noted that the computed values for σ^2 incorporate both dynamic and static disorder, the latter being related to crystal defects and crystal size. Summarizing, we conclude that all bone samples consist of disordered hydroxyapatite and possess the same local structure on a sub-nanometer scale.

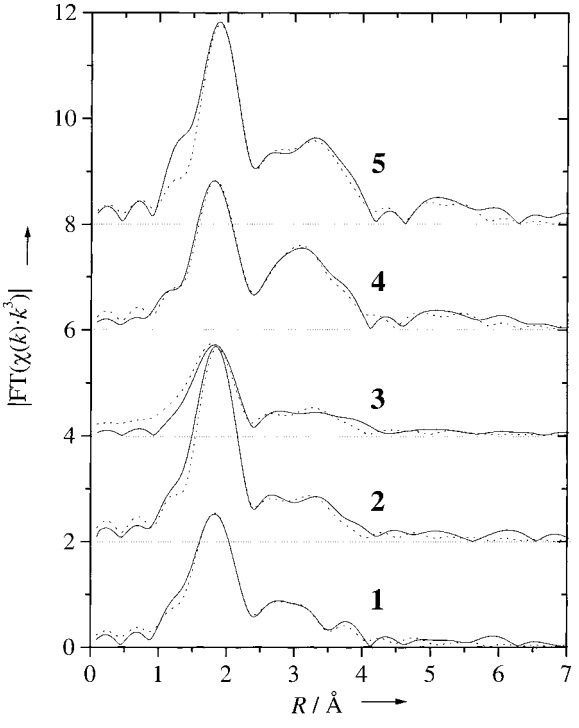

Fig. 4. Fourier-transform magnitudes of five samples (Ca K-edge), showing the short-range environment of calcium in the samples. The first shell around calcium (oxygen, around 2 Å) is comparable in all cases. The main difference is found in the higher shells (2.5–4.5 Å) that are strongly disordered for the biological samples (bottom) as compared to crystalline hydroxyapatite and endobon. Note that the distances displayed on the *x*-axis were not corrected for phase shifts, i.e. they all appear 0.2–0.3 Å too small (solid lines, experimental data; and dotted lines, fit to the data). 1, Tumor bone; 2, callus bone; 3, Kiel bone; 4, endobon; and 5, synthetic hydroxyapatite.

Table 3
Quantitative evaluation of EXAFS data[a]

Shell	Ca-6 O	Ca-2.4 P	Ca-2.4 P	Ca-6 Ca	Ca-2.4 Ca	Ca-3.6 Ca
Hydroxyapatite/crystallographic values[b]	2.32/2.41	3.03/3.36	3.46/3.67	3.99/4.08	4.17	5.45/5.84
Hydroxyapatite (synthetic)	2.42/10	3.16/10	3.65/32	4.05/8	4.26/3	5.86/7
Kiel bone	2.40/20	3.16/20	3.66/40	3.92/23	4.17/14	5.68/36
Callus bone	2.41/9	3.18/14	3.64/16	3.91/50	4.15/13	5.81/19
Tumor bone	2.41/14	3.18/15	3.65/18	3.94/30	4.18/13	5.80/24
Endobon®	2.41/12	3.19/12	3.66/10	4.00/20	4.17/6	5.85/7

[a] Given for each shell are: distance (Å) and Debye–Waller factor $\sigma^2 \times 1000$ (Å^2). All samples can be fitted to a hydroxyapatite model.
[b] This row shows the computed crystallographic parameters for ideally crystalline hydroxyapatite [13].

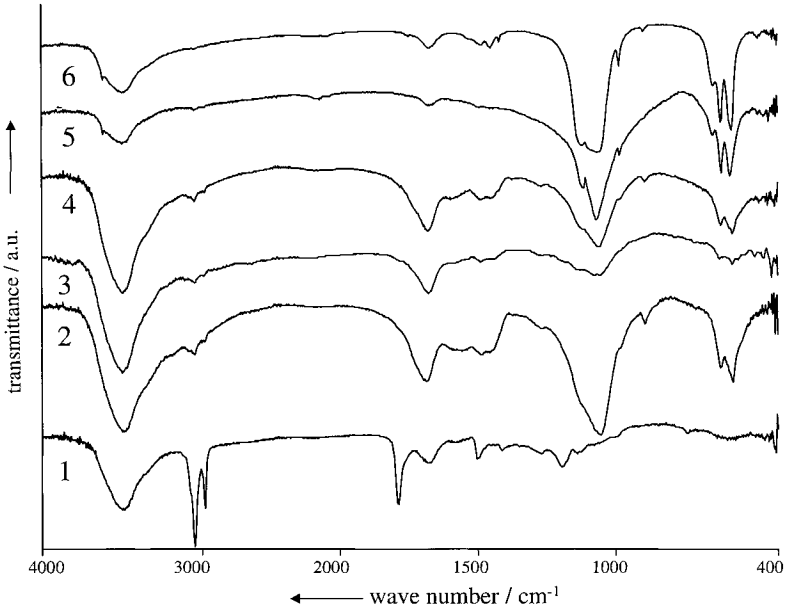

Fig. 5. Infrared spectra of different samples. 1, Spongiosa B; 2, tumor bone; 3, callus bone; 4, Kiel bone; 5, endobon; and 6, synthetic hydroxyapatite.

The results from IR spectroscopy (Fig. 5) confirm those obtained by diffraction and thermal analysis: endobon is well crystallized whereas natural bone samples and Kiel bone contain disordered crystallites. The carbonate and organic tissue can be detected as well. Hydroxyapatite shows the following characteristic bands: 1028–1100 cm^{-1} (ν_3 [′,″,‴], P–O stretch), 960 cm^{-1} (ν_1 sym, P–O stretch), 603 cm^{-1} (ν_4‴, P–O stretch), 564 cm^{-1} (ν_4″, P–O stretch and P–O bending). The band at 1028–1100 cm^{-1} is indicative of the crystallinity: Hydroxyapatite shows two bands while amorphous calcium phosphate (ACP) shows a broad single band. Substituted carbonate gives rise to a band at 1400–1450 cm^{-1} (ν_3) and leads also to coalescence of the two bands at 1028–1100 cm^{-1} [31]. Occluded water gives two bands at 3500 cm^{-1} (ν_s) and 1630 cm^{-1} (δ_{OH}). We note the following effects:

- Endobon and hydroxyapatite are highly crystalline, as shown by the band-splitting at 1030–1100 cm^{-1}. However, carbonate is included in commercial hydroxyapatite, as shown by the double band at 1400–1450 cm^{-1}, whereas endobon contains no carbonate, thus confirming the thermogravimetric results.
- Kiel bone, tumor bone and callus bone contain hydroxyapatite with medium crystallinity. The carbonate content appears to be higher in Kiel bone and tumor bone as compared to callus bone. Qualitatively, the intensity of the apatite bands matches the mineral content as found by thermogravimetry.
- In spongiosa B, the vibration bands of apatite are barely visible. We attribute this to the high content of organic matrix (collagen, fat tissue) which masks the features of the mineral phase. Note that the IR spectrum was taken from a representative aliquot of the sample, i.e. it includes both soft tissue and hard tissue.

4. Discussion

All studied natural bone samples, although they have a very different history, contain mineral particles of disordered carbonated hydroxyapatite of the same morphology and size. The chemical composition of the bone samples is variable with respect to the total mineral content (carbonated apatite) and the carbonate content in the mineral phase. Further studies are

necessary to relate the carbonate content and the mineral content to bone history and function. Apparently, in biosynthesis, size and shape of the bone mineral phase are kept constant whereas its chemical composition is not.

In order to develop a clinically useful bone substituent material, many attempts have been made to match the biocompatibility of autologous bone. Kiel bone (sterilized bone) contains the same crystallites as natural bone, but they are accompanied by the immunogenic organic collagen matrix. The bone substituent material endobon (calcined bone) consists of highly crystalline, carbonate-free hydroxyapatite without any organic components. The good biocompatibility of hydroxyapatite is known. However, endobon is resorbed very slowly in the body (little participation in remodeling).

We offer the following explanation: the crystals in endobon are in a thermodynamically very stable state that causes very slow resorption. The comparatively fast remodeling process occurring in living bone is facilitated by the presence of extremely small, disordered and carbonate-substituted hydroxyapatite crystals far from thermodynamic equilibrium. They possess a higher specific energy, therefore their solubility is higher than that of compact, well crystalline hydroxyapatite, and osteoclastic resorption in local acidic compartments is enhanced. For an ideal bone substituting material, one would have to combine the small higher-energy carbonate apatite crystallites with an absence of possibly immunogenic organic tissue.

Acknowledgements

We are grateful to Prof. Dr. G. Delling (Hamburg) for providing the bone samples and for histological analysis. We thank H. Ehrenberg (Hamburg) for help with the synchrotron X-ray diffraction experiments. Synchrotron beamtime was generously allocated by HASYLAB at DESY. We thank J. M. Rueger (Hamburg) and H.J. Kock (Darmstadt) for making available the sample of endobon.

References

[1] S. Mann, G.A. Ozin, Nature 382 (1996) 313.
[2] S.I. Stupp, P.V. Braun, Science 277 (1997) 1242.
[3] R.A. Robinson, John Hopkins Med. J. 145 (1979) 10.
[4] S. Weiner, H.D. Wagner, Annu. Rev. Mater. Sci. 28 (1998) 271.
[5] T. Ichijo, Y. Yamashita, T. Terashima, Bull. Tokyo Med. Dent. Univ. 40 (2) (1993) 93.
[6] V. Ziv, H.D. Wagner, S. Weiner, Bone 18 (1996) 417.
[7] U. Plate, S. Arnold, T. Kotz, U. Stratmann, H.P. Wiesmann, H.J. Höhling, Connective Tissue Res. 38 (1998) 149.
[8] P. Schaller, Osteosynthese International 2 (1994) 177.
[9] U. Saalfeld, N.M. Meenen, T.T. Jüres, H. Saalfeld, Biomaterials 15 (1994) 905.
[10] A. Boyde, S.J. Jones, Microsc. Res. Technol. 33 (1996) 92.
[11] E.A. Stern, M. Newville, B. Ravel, Y. Yacoby, D. Haskel, Physica B 208-209 (1995) 117.
[12] J.J. Rehr, R.C. Albers, S.I. Zabinsky, Phys. Rev. Lett. 69 (1992) 3397.
[13] A.S. Posner, A.F. Diorio, Acta Cryst. 11 (1958) 308.
[14] R.Z. Legeros, O.R. Trautz, J.P. Legeros, E. Klein, Bull. Soc. Chim. Fr. (1968) 1712.
[15] J.C. Elliot, Structure and Chemistry of the Apatites and Other Calcium Orthophosphates, Vol. 18, Elsevier, Amsterdam, 1994.
[16] J.M. Lane, F. Betts, A.S. Posner, D.W. Yue, J. Bone Joint Surg. Am. 66 (1984) 1289.
[17] E.P. Paschalis, F. Betts, E. DiCarlo, R. Mendelsohn, A.L. Boskey, Calcif. Tissue Int. 61 (1997) 480.
[18] E.F. Kaelble, McGraw–Hill, 1967.
[19] R.Z. Legeros, Nature 206 (1965) 403.
[20] L.W. Fisher, E.D. Eanes, L.J. Denholm, B.R. Heywood, J.D. Termine, Calcif. Tissue Int. 40 (1987) 282.
[21] R.Z. Legeros, J.P. Legeros, in: J.O. Nriagu, P.B. Moore (Eds.), Phosphate Minerals, Springer, Berlin, 1984, Chapter 12.
[22] D.J. Simmons, J.E. Russel, M.D. Grynpas, Bone Mineral 1 (1986) 485.
[23] V. Ziv, I. Sabanay, T. Arad, W. Traub, S. Weiner, Microscop. Res. Technol. 33 (1996) 203.
[24] G. Bocchi, G. Valdre, J. Inorg. Biochem. 49 (1993) 209.
[25] H. Bertagnolli, T.S. Ertel, Angew. Chem. Int. Ed. Engl. 33 (1994) 45.
[26] J.E. Harries, D.W.L. Hukins, S.S. Hasnain, Calcif. Tissue Int. 43 (1988) 250.
[27] J.E. Harries, D.W.L. Hukins, C. Holt, S.S. Hasnain, J. Cryst. Growth 84 (1987) 563.
[28] M.G. Taylor, K. Simkiss, J. Simmons, L.N.Y. Wu, R.E. Wuthier, Cell. Mol. Life Sci. 54 (1998) 192.
[29] J.E. Harries, D.W.L. Hukins, S.S. Hasnain, J. Phys. C: Solid State Phys. 19 (1986) 6859.
[30] S. Sugiyama, T. Minami, T. Moriga, H. Hayashi, K. Koto, M. Tanaka, J.B. Moffat, J. Mater. Chem. 6 (1996) 459.
[31] C. Rey, V. Renugopalakrishnan, B. Collins, M.J. Glimcher, Calcif. Tissue Int. 49 (1991) 251.